Supplementary Information (SI) for Inorganic Chemistry Frontiers.

In Situ Reconstructed CuO_x–BTA Heterointerface Enables Stable and Stable Nitrate Electroreduction to Ammonia

Meng Wang, †[ab] Yuyin Mao, †[b] Xiangdong Xue,[b] Yucheng Dong,[b] Xinjiao Cao,[b] Qing Dong, [b] Weiqiang Tan*[a] and Jian Liu*[b]

a. College of Environmental and Municipal Engineering, Qingdao University of Technology, Qingdao 266520, P. R. China

b. State Key Laboratory of Photoelectric Conversion and Utilization of Solar Energy, Qingdao New Energy Shandong Laboratory, Qingdao Institute of Bioenergy and Bioprocess Technology, Chinese Academy of Sciences, Qingdao 266101, P. R. China

#Both authors contributed equally

E-mail: tanweiqiang@qut.edu.cn

E-mail: liujian@qibebt.ac.cn

Experimental Section

Preparation of working electrodes

10 mg of Cu-BTA powder was dispersed in a mixture of 1.5 mL deionized water and 0.5 mL isopropanol by ultrasonication for 30 minutes. Then, 50 μL of Nafion 117 perfluorinated resin solution was added to the suspension, followed by an additional 30 minutes of ultrasonication to obtain a homogeneous catalyst ink. 200 μL of ink was sprayed onto a carbon paper (0.5 cm × 1 cm) to fabricate the working electrode, with the loading amount of the catalyst being approximately 2.0 mg per square centimeter. The preparation processes of the CuNPs electrode (XFNANO, Copper Nanopowder: 150-200 nm) and Cu_2O electrode (Aladdin, Cuprous Oxide, ≥99%) used for comparison were the same as described above, with commercially available chemicals serving as comparative catalysts.

In situ Fourier transform-infrared absorption (FT-IR) spectroscopy measurements

In situ FT-IR spectroscopy measurements were conducted using a FT-IR spectrometer (Bruker VERTEX 70V). The electrochemical experiments employed a three-electrode cell setup with an electrolyte comprising 0.1 M KNO_3 and 1 M KOH. The spectral resolution was set at 4 cm^{-1}, and spectra recorded at open circuit potential (OCP) served as reference points. Measurements were taken across a potential range from −0.08 V to −0.88 V vs. RHE. To enhance signal sensitivity, a monocrystalline silicon substrate with a gold-plated surface was utilized. The scanning range spanned from 4000 cm^{-1} to 400 cm^{-1}.

In situ Raman measurement

Raman spectra were collected using a Renishaw in Via microprobe Raman spectrometer, employing an excitation laser at 532 nm with 3 mW between 200 and 1900 cm^{-1}. The working electrode (1 × 1 cm^2) was immersed in the electrolyte solution consisting of 1 M KOH and 0.1 M KNO_3. Hg/HgO electrode served as the reference electrode, while a platinum wire functioned as the counter electrode. The electrochemical measurements at −0.68V vs. RHE were performed intermittently, and in situ Raman experiments were carried out continuously throughout the procedure.

XAFS measurements and analysis

XAFS analyses were performed with Si (111) crystal monochromators at the beamline 7-lD of the Advanced PhotonSource (APS) at Argonne National Laboratory. The EXAFS spectra were recorded in

transmission mode. The acquired EXAFS data were processed according to the standard procedures using the Athena program implemented in the IFEFFIT software packages. The normalized EXAFS spectra were obtained by setting the pre-edge and post-edge to 0 and 1, respectively. Then, the χ (k) data were Fourier transformed into real (R) space by a Hanning window with sill size of 1.0 Å−1 to separate the EXAFS contributions from the distinct coordination shells. To obtain quantitative structural parameters around Ni atoms, least-squares curve parameter fitting was performed using the ARTEMIS module of the IFEFFIT software packages.

Nuclear Magnetic Resonance Spectroscopy

The ^{1}H NMR spectra were obtained using a Bruker AVANCE III 600 spectrometer. A mixture of 0.5 mL dimethyl sulfoxide-d_6 and 1 mL standard solution was prepared, and the pH was adjusted to 2.0 using 1 mL of 2 M HCl before transferring to an NMR tube. The concentrations of $^{14}NH_4^+/^{15}NH_4^+$ in the sample were determined by comparing the triplet/doublet signals of ammonium with the singlet signal of dimethyl sulfoxide-d_6.

Product Quantification.

The ionic concentrations in the electrolyte were analyzed using a Hitachi U-3900 UV–vis spectrophotometer. Prior to measurement, electrolyte samples were diluted as necessary to ensure that their concentrations fell within the linear range of the calibration curves.

Quantification of NH_4^+.

For ammonia quantification, 50 μL of the electrolyte was withdrawn from the reaction cell and diluted to 4 mL with deionized water. Subsequently, 2 mL of 1 M NaOH solution containing salicylic acid and sodium citrate, 1 mL of 0.05 M NaClO solution, and 0.2 mL of 1 wt.% sodium nitroferricyanide solution were sequentially added to the mixture and thoroughly mixed. The mixture was allowed to react at room temperature for 2 hours, after which the UV–vis absorption spectrum was recorded. The absorbance at 650 nm was used to determine the NH_4^+ concentration. A calibration curve was constructed using a series of standard ammonium chloride solutions processed under identical conditions.

Quantification of NO_2^-.

To prepare the colorimetric reagent, 4 g of sulfanilamide, 0.2 g of N-(1-naphthyl) ethylenediamine

dihydrochloride, and 10 mL of phosphoric acid (1.7 g mL^{-1}) were dissolved in 50 mL of ultrapure water. For nitrite quantification, 20 μL of the electrolyte was diluted to 4 mL with deionized water, then 0.1 mL of the prepared colorimetric reagent was added. After thorough mixing, the solution was left to stand for 20 minutes. The absorbance at 540 nm was measured to determine the NO_2^- concentration. A calibration curve was established using a series of standard sodium nitrite solutions treated in the same manner.

Quantification of NO_3^-.

Take 20 μL of the sample solution and dilute it to 8 mL. Add 160 μL of 1 M HCl and 16 μL of 0.8 wt% sulfamic acid solution. Allow the mixture to stand for 20 minutes, then measure the absorbance at wavelengths of 220 nm and 275 nm. The nitrate concentration is determined from the difference in absorbance at these two wavelengths.

Quantification of N_2H_4.

The colorimetric reagent was prepared by dissolving 6 g of p-dimethylaminobenzaldehyde in a mixture of HCl (30 mL) and ethanol (300 mL). Subsequently, 20 μL of cathodic electrolyte was diluted to 2.5 mL and mixed with 2.5 mL of the prepared colorimetric reagent. The mixture was then incubated at room temperature in the dark for 20 minutes. The UV-Vis absorption spectrum was measured, and the absorbance at 458 nm was recorded. A calibration curve was established using a series of standard N_2H_4 solutions processed in the same manner.

Calculation of copper leaching amount

The formula for calculating the copper leaching amount is as follows：

$$K_{Cu} = \frac{C_m \times V}{S \times P \times I} \times 100\%$$

Where *Cm* is the dissolution concentration of Cu (ppm), *V* is the volume of the electrolyte (0.02L), *S* is the electrode area (0.5cm²), *P* is the electrode load (2mg/cm²), *I* is the mass percentage of Cu in Cu-BTA (0.32).

K=1.18%

DFT method

All structural optimizations and energy evaluations were carried out via spin-polarized density functional

theory (DFT) within the CP2K package.[1] The exchange–correlation effects were treated using the generalized gradient approximation with the Perdew–Burke–Ernzerhof (PBE) functional,[2] supplemented with Grimme's DFT-D3 empirical dispersion correction.[3] Core electrons were represented by the Goedecker–Teter–Hutter (GTH) pseudopotentials,[4-5] while valence electrons were expanded in a double-ζ valence polarization basis sets optimized for molecules and short-range (DZVP-MOLOPT-SR-GTH),[6] minimizing basis set superposition errors. A plane-wave cutoff of 600 Ry was applied for the auxiliary basis. Geometry optimizations were performed using the Broyden–Fletcher–Goldfarb–Shanno (BFGS) algorithm, with forces converged to within 4.5×10^{-4} Hartree/Bohr. Thermodynamic properties were subsequently computed based on the optimized structures, and analyzed by Shermo software.[7] The CP2K input file was generated using the Multiwfn.[8-9]

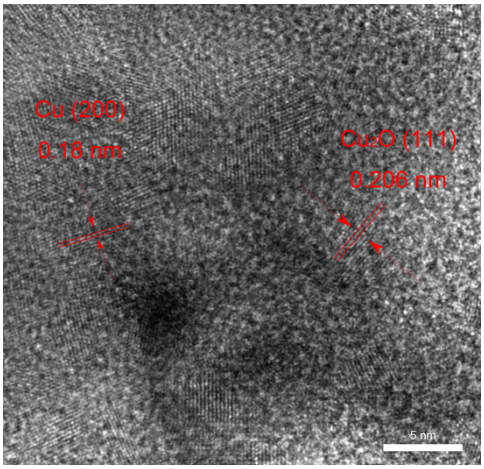

Fig. S1. The TEM images of CuO_x-BTA.

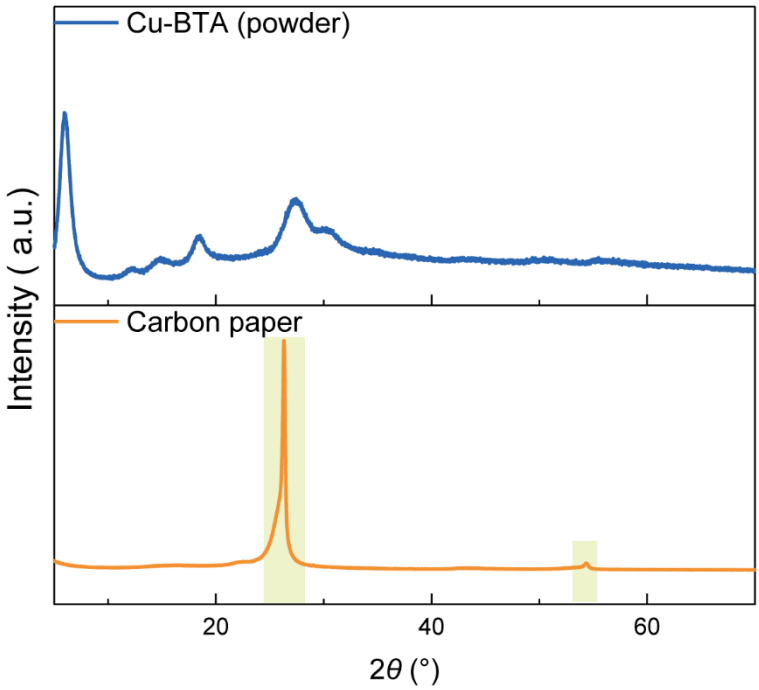

Fig. S2. (a) XRD patterns of Cu-BTA (powder); (b) XRD pattern of hydrophilic carbon paper.

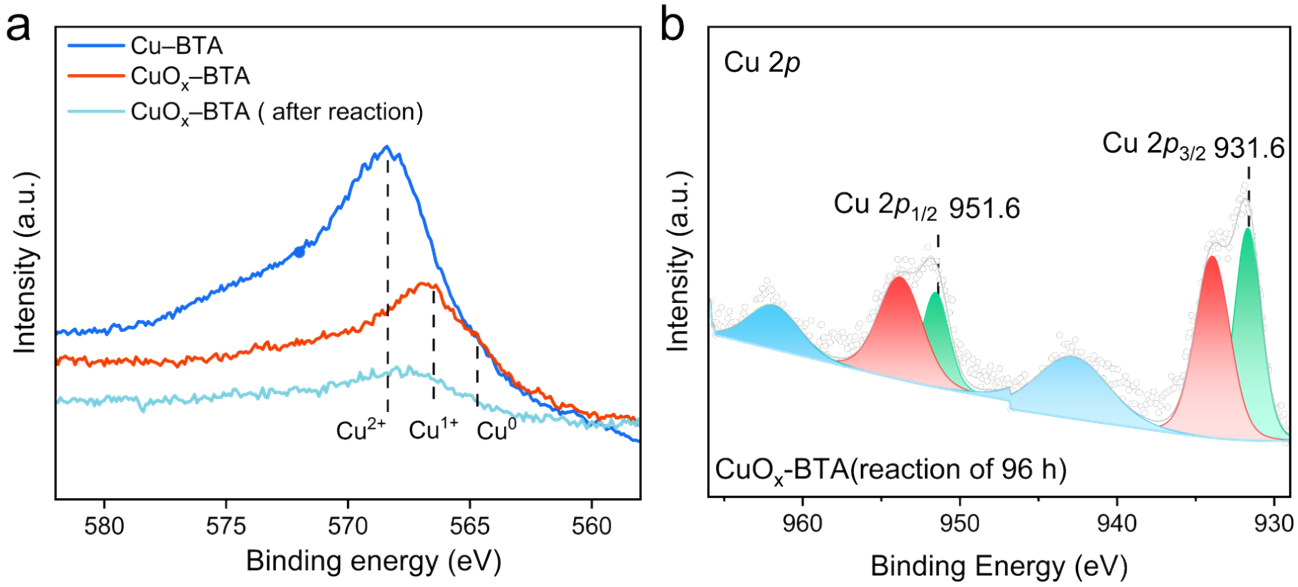

Fig. S3. (a) XPS Cu LMM spectra comparing Cu-BTA and CuOx-BTA. (b) XPS Cu *2p* spectra after the CuO_x-BTA reaction for 96 hours.

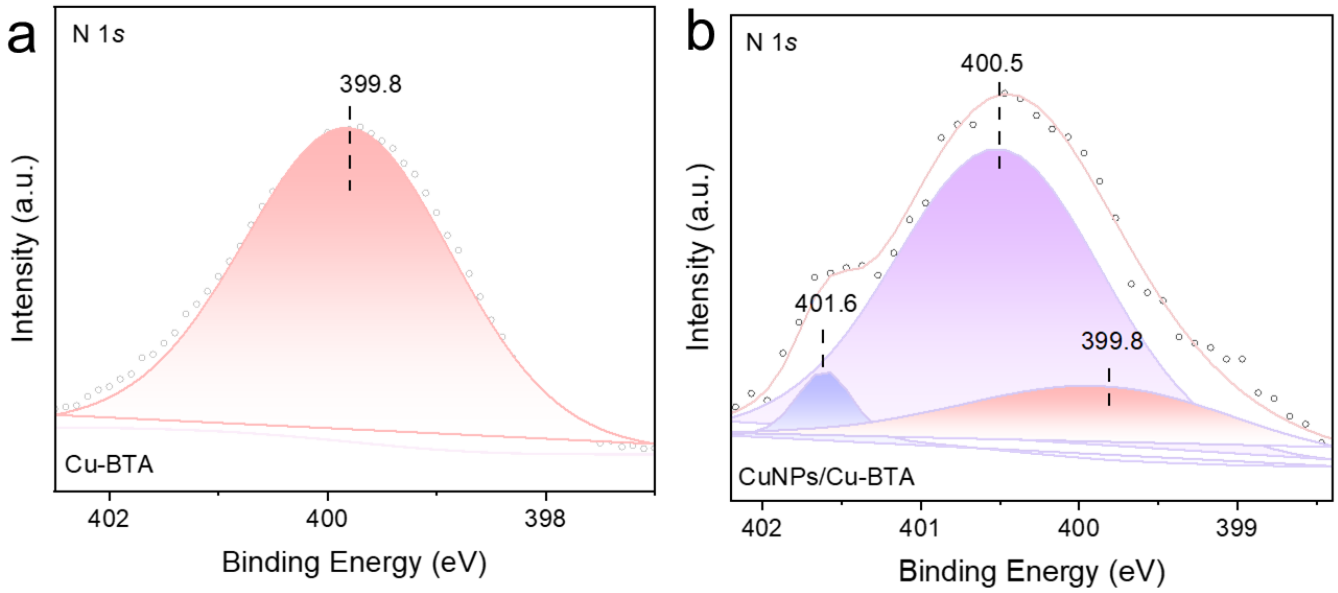

Fig. S4. XPS N *1s* spectra of (a) Cu-BTA and (b) CuO_x-BTA.

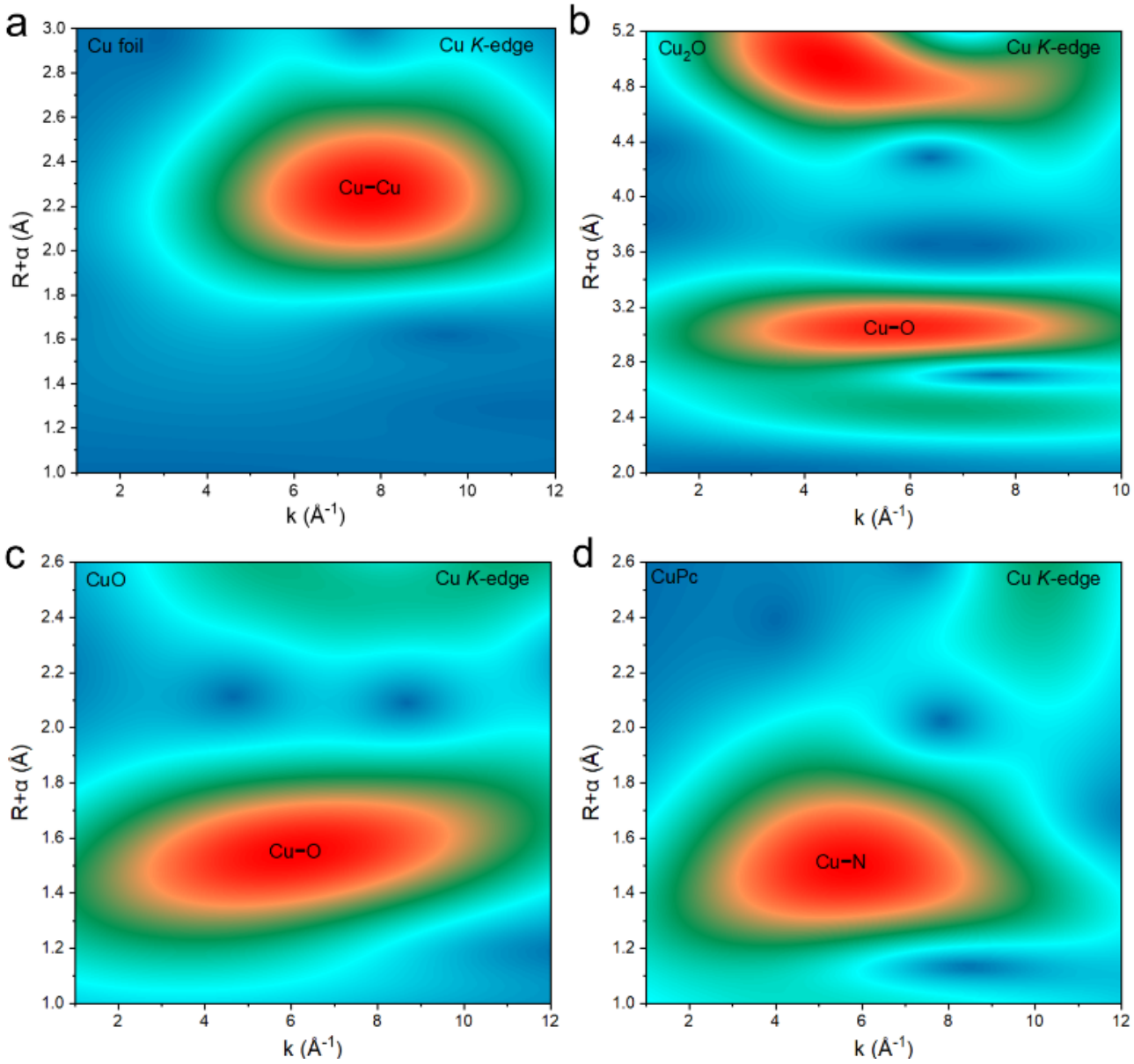

Fig. S5. Wavelet transform analysis of the k³-weighted EXAFS spectra for (a) Cu foil, (b) Cu_2O (b) CuO and (d) CuPc.

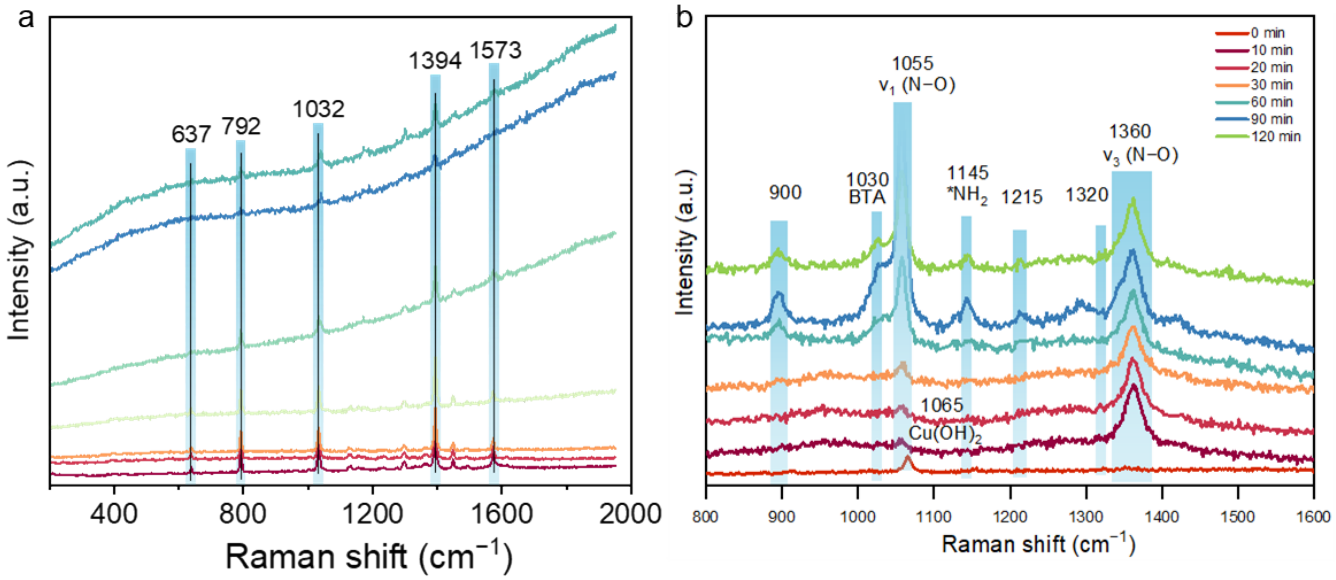

Fig. S6. In situ Raman spectrum of (a) Cu-BTA (1h) and (b) CuO_x-BTA (2h) surface at −0.68 V.

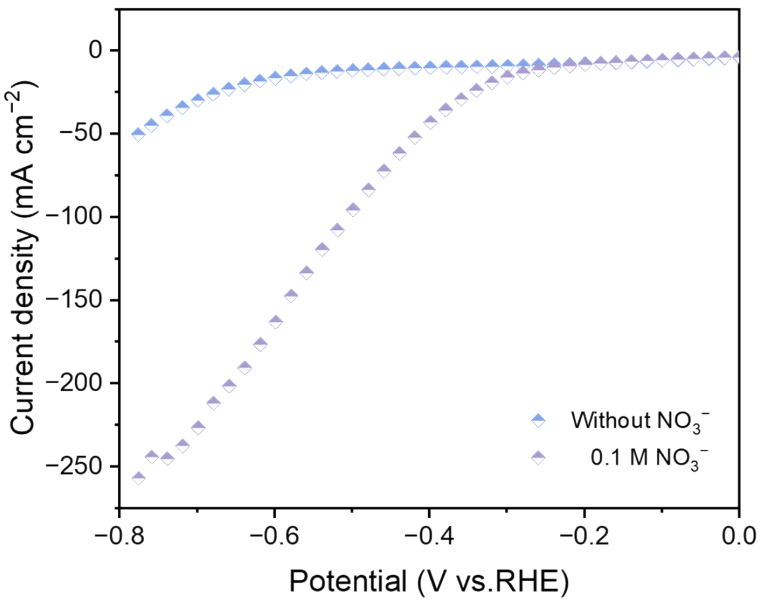

Fig. S7. Comparison of LSV curves in electrocatalytic reduction with 0.1 M NO_3^- and without NO_3^-.

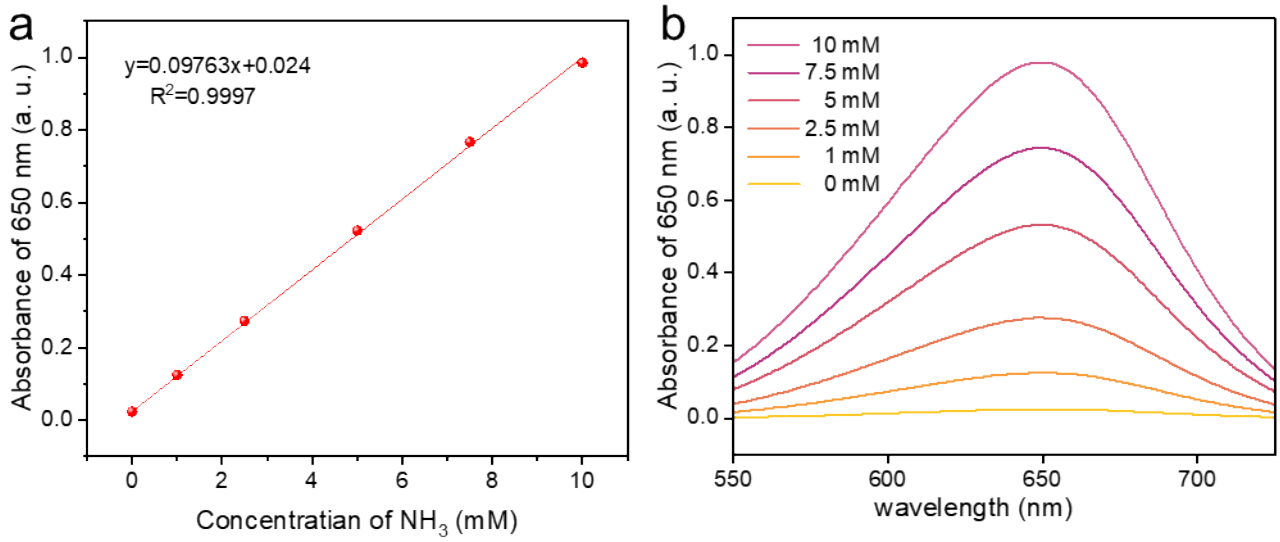

Fig. S8. (a) Calibration curve used for estimating concentrations of NH_3. (b) UV-vis spectra of various NH_3 concentrations.

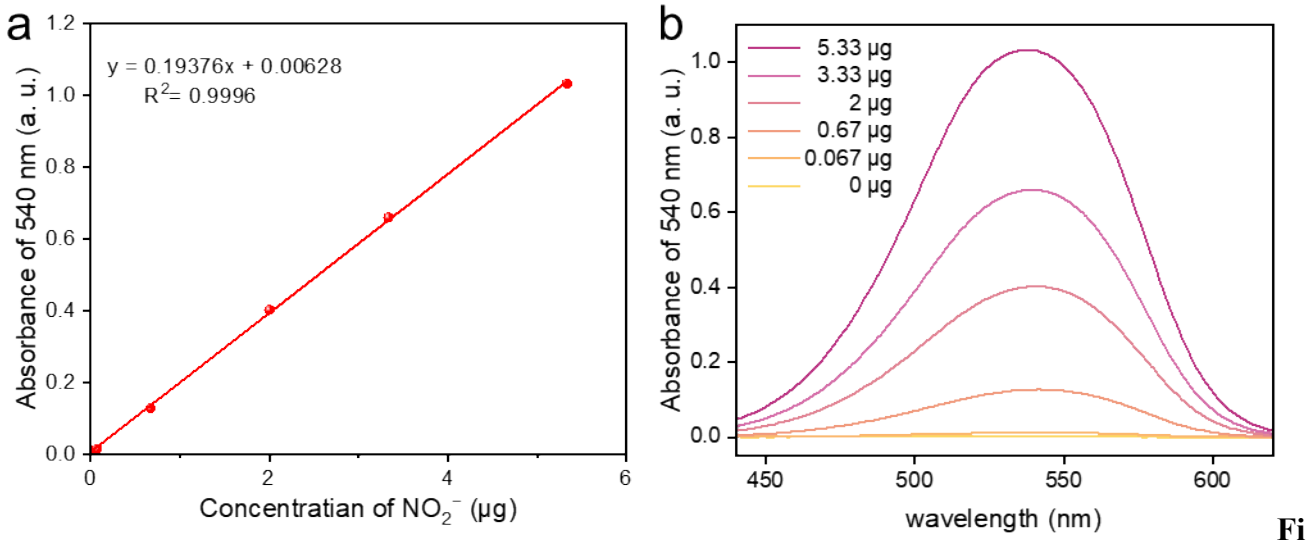

Fig. S9. (a) Calibration curve used for estimating concentrations of NO_2^-. (b) UV-vis spectra of various NO_2^- concentrations.

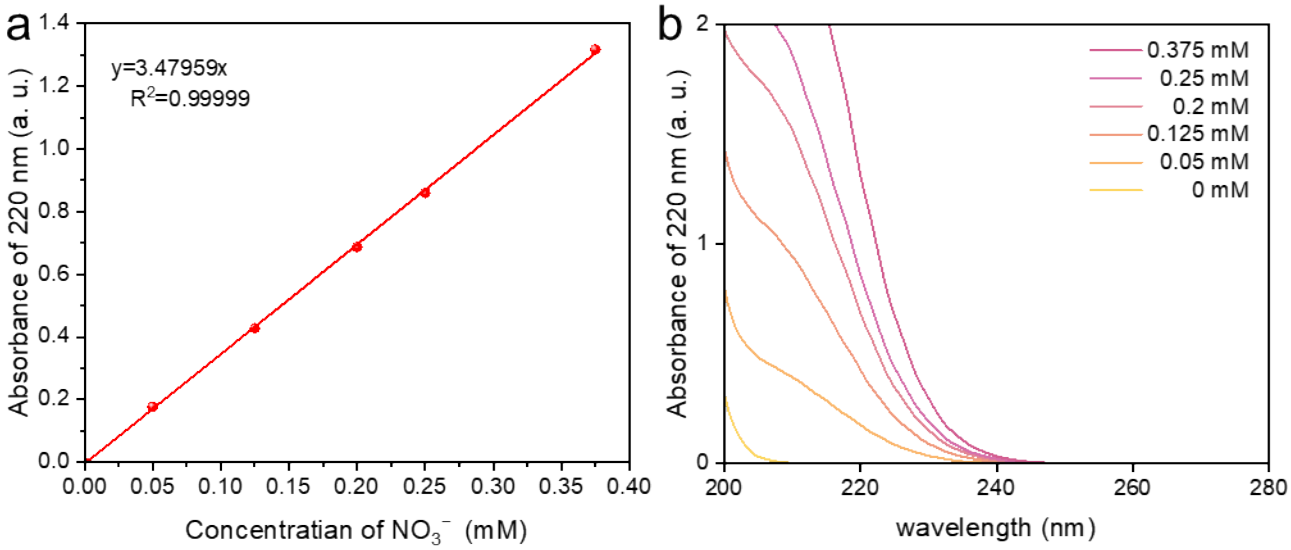

Fig. S10. (a) Calibration curve used for estimating concentrations of NO_3^-. (b) UV-vis spectra of various NO_3^- concentration.

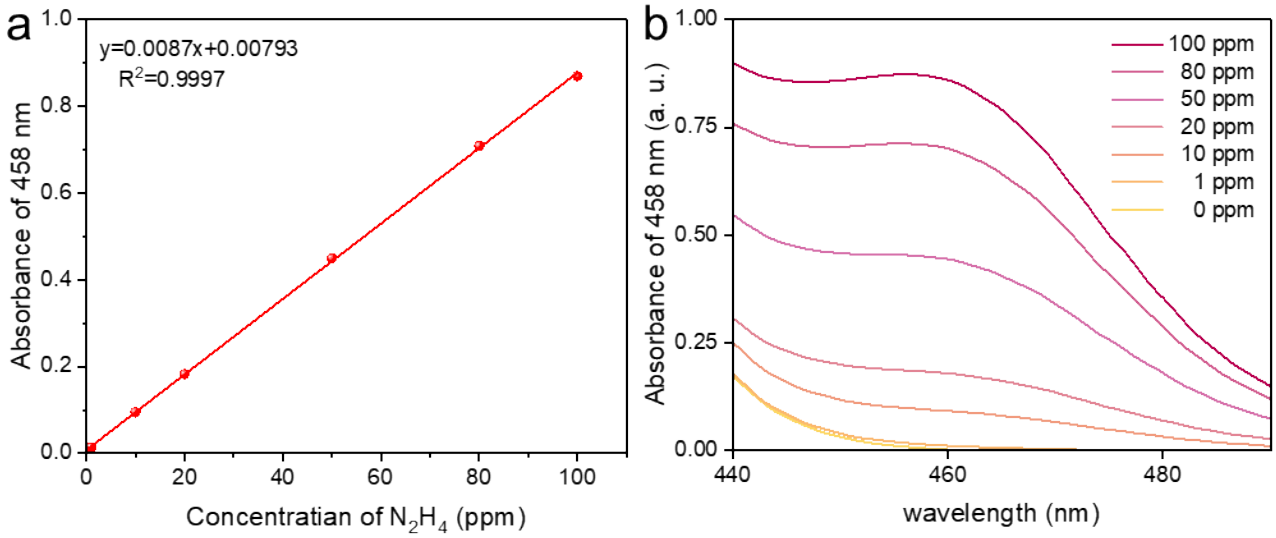

Fig. S11. (a) Calibration curve used for estimating concentrations of N_2H_4. (b) UV-vis spectra of various N_2H_4 concentration.

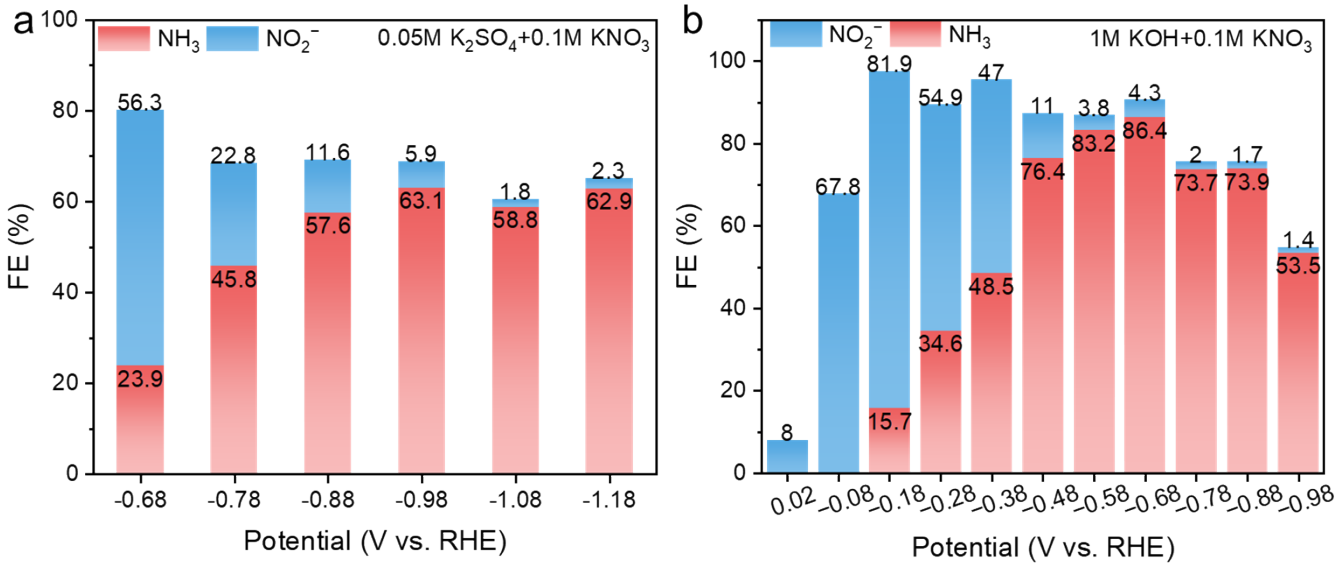

Fig. S12. The Faradaic efficiency of the reconstruction process for Cu-BTA in 0.05 M K_2SO_4 + 0.1 M KNO_3 (pH = 7) and 1 M KOH + 0.1 M KNO_3 (pH = 14).

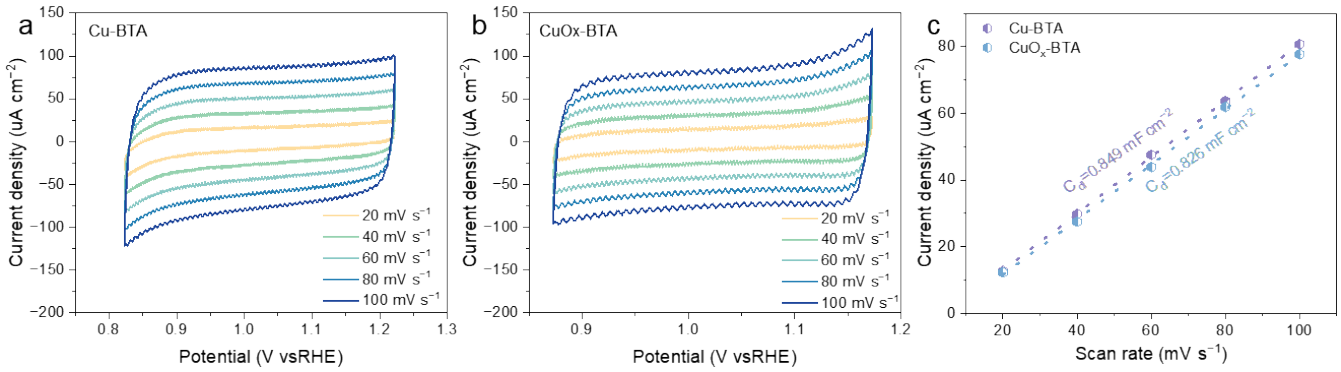

Fig. S13. The CV curves of (a) Cu-BTA and (b) CuO_x-BTA with various scan rates from 20 to 100 mV s^{-1}. (c) Plots of the current density versus the scan rate for Cu-BTA and CuO_x-BTA.

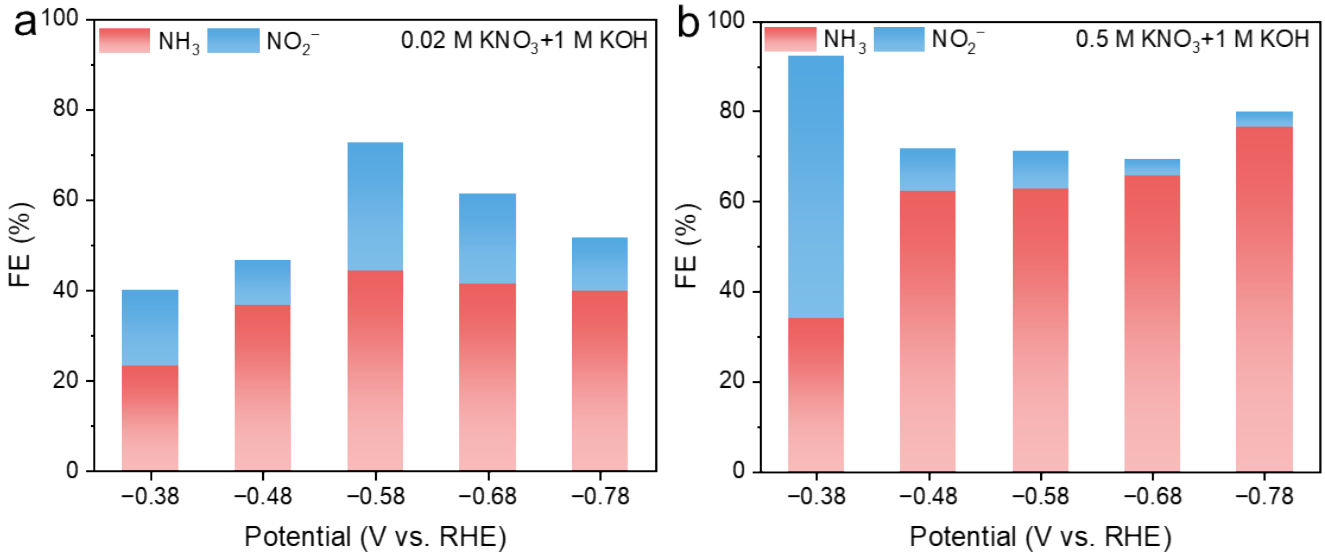

Fig. S14. (a) Faradaic efficiency of CuO_x-BTA at different reduction potentials in 0.02 M NO_3^-+1 M KOH and (b) 0.5 M NO_3^-+1 M KOH.

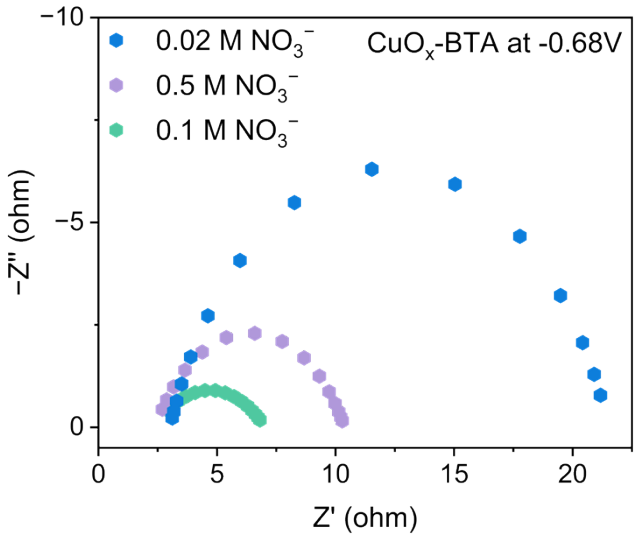

Fig. S15. The Nyquist plots of CuO_x-BTA at different concentrations at −0.68V.

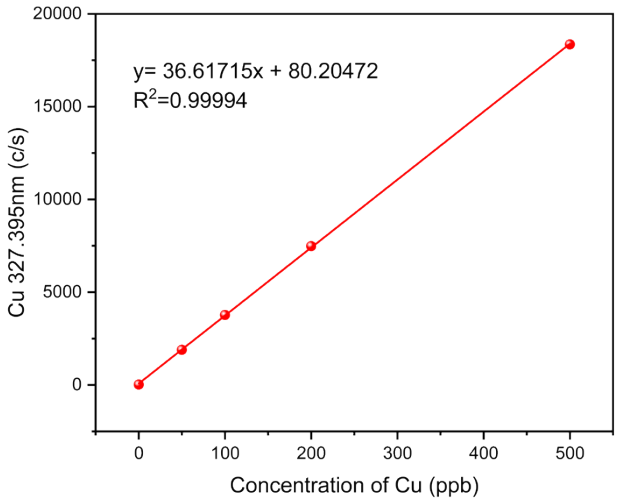

Fig. S16. The standard calibration curve for copper (Cu) in ICP analysis was established using a series of standard solutions with known Cu concentrations.

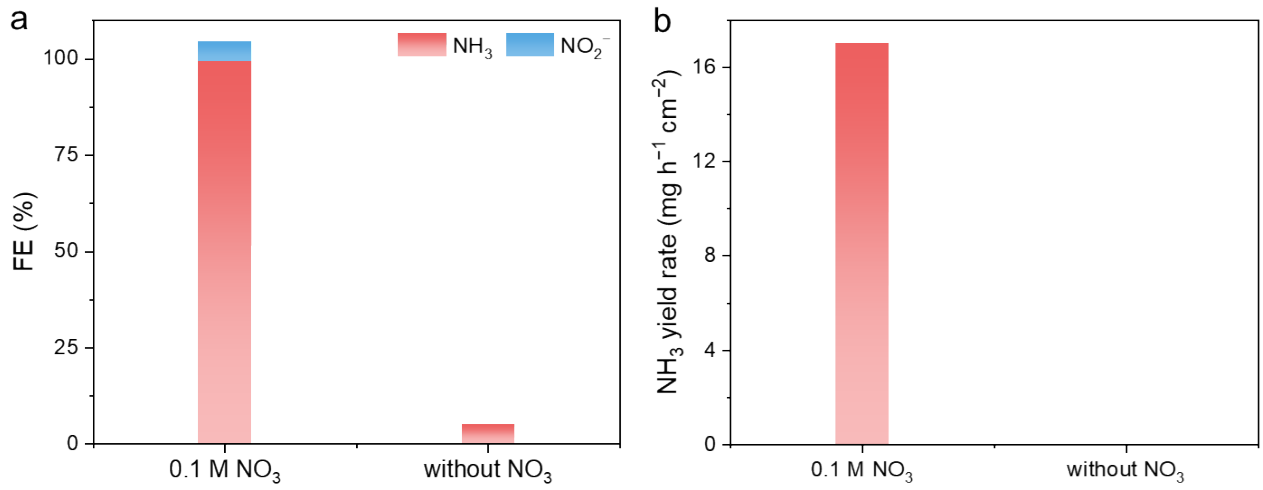

Fig. S17. Comparison of (a) Faradaic efficiency and (b) ammonia yield in electrocatalytic reduction with and without nitrate in the electrolyte.

Table S1. The ICP testing data for Cu leaching of CuO_x–BTA after reacting in the electrolyte for 96 hour.

Sample	concentration (ppb)	intensity (c/s)
1	**190**	**6953.22**
2	**190**	**7108.37**
3	**190**	**7232.64**

Table S2. The fitting parameters of Cu *K*-edge Fourier-filtered k^3-weighted EXAFS for various samples.

Samples	Path	CN	R (Å)	ΔE_0 (eV)	S_0^2	σ^2 (Å^2)	*R*-factor
1	Cu−N	3.9±0.1	1.51±0.02	3.2±0.21	0.90	0.0033±0.0046	0.0018
2	Cu−N	2.2±0.2	1.53±0.02	5.1±0.19	0.90	0.0037±0.0034	0.0011

CN: coordination numbers, R: bond distance, ΔE_0: the inner potential correction; σ^2: Debye-Wallerfactors, R-factor: goodness of fit. S_0^2 was fixed as 0.90. Data ranges: $3 \leq k \leq 12$ Å^{-1}, $1.0 \leq R \leq 3.0$ Å.

Reference

1. Hutter, J.; Iannuzzi, M.; Schiffmann, F.; VandeVondele, J., CP2K: atomistic simulations of condensed matter systems. *Comput. Mol. Sci.* **2013,** *4* (1), 15–25.
2. Perdew, J. P.; Burke, K.; Ernzerhof, M., Generalized gradient approximation made simple. *Phys. Rev. Lett.* **1996,** *77*, 3865–3868.
3. Grimme, S., Semiempirical GGA-type density functional constructed with a long-range dispersion correction. *J. Comput. Chem.* **2006,** *27* (15), 1787–1799.
4. Goedecker; Teter; Hutter, Separable dual-space Gaussian pseudopotentials. *Phys. Rev. B* **1996,** *54*, 1703–1710.
5. Hartwigsen, C.; Goedecker, S.; Hutter, J., Relativistic separable dual-space Gaussian pseudopotentials from H to Rn. *Phys. Rev. B* **1998,** *58* (7), 3641–3662.
6. VandeVondele, J.; Hutter, J., Gaussian basis sets for accurate calculations on molecular systems in gas and condensed phases. *J. Chem. Phys.* **2007,** *127*, 114105.
7. Lu, T.; Chen, Q., Shermo: A general code for calculating molecular thermochemistry properties. *Comput. Theor. Chem.* **2021,** *1200*, 113249.
8. Lu, T.; Chen, F., Multiwfn: A multifunctional wavefunction analyzer. *J. Comput. Chem.* **2011,** *33*, 580–592.
9. Lu, T., A comprehensive electron wavefunction analysis toolbox for chemists, Multiwfn. *J. Chem. Phys.* **2024**, 082503.